Length mismatch in random semiconductor alloys. IV. General multinary compounds

R. W. Wang and M. F. Thorpe
Department of Physics and Astronomy, Michigan State University, East Lansing, Michigan 48824
and Center for Fundamental Materials Research, Michigan State University, East Lansing, Michigan 48824

Normand Mousseau
Theoretical Physics, University of Oxford, 1 Keble Road, OX1 3NP Oxford, United Kingdom
(Received 17 July 1995)

We generalize previous theory on the length-mismatch problem in random semiconductor alloys to deal with an *arbitrary* number of components on each sublattice. We also calculate the length-distribution functions for *any* two sites in the crystalline alloy. It is found that the properly scaled length-distribution functions are independent of the types of atomic species, and the first and second moments of the distributions are calculated. We illustrate these results with computer simulations performed on Si_xGe_{1-x}, and apply these results to the pseudoternary alloy $Cd_{1-x-y}Mn_xZn_yTe$.

I. INTRODUCTION

Structural information on semiconducting materials is of fundamental importance in calculating, predicting, and understanding a wide range of their properties.[1-3] For example, the interactions between the magnetic ions (Mn) in the semiconducting alloy $Cd_{1-x-y}Mn_xZn_yTe$ depends sensitively on the Mn-Mn spacing,[4] thus it is important to understand the bond-length distributions in these multinary alloys. As the fourth of the series on length mismatch in random alloys, this paper generalizes the previous approach[5] to deal with a compound with the generic formula $\{(A_\alpha)_{x_\alpha}\}\{(B_\beta)_{y_\beta}\}$ (where $\alpha=1,\ldots,N$, $\sum_\alpha x_\alpha=1$; and $\beta=1,\ldots,M$, $\sum_\beta y_\beta=1$). We also calculate the length-distribution functions for *any* two sites in the crystalline alloy. We find that the scaled length-distribution functions are independent of the types of atomic species in question, and the first and second moments of the distributions are calculated. The results for more distant pair distributions are illustrated with computer simulations performed on Si_xGe_{1-x}, where each sublattice of the zinc-blende structure is populated by a random mixture of Si and Ge with the same stoichiometric formula Si_xGe_{1-x}, such that in the language above, $N=M=2$, $A_1=B_1=$Si, $A_2=B_2=$Ge, $x_1=y_1=x$, and $x_2=y_2=1-x$. The theory is also applied to the pseudoternary alloy $Cd_{1-x-y}Mn_xZn_yTe$, where we may identify $N=3$, $A_1=$Cd, $x_1=1-x-y$, $A_2=$Mn, $x_2=x$, $A_3=$Zn, $x_3=y$; and $M=1$, $B_1=$Te, $y_1=1$. The pair distribution function (PDF) in simulations is a structural property of the material that can be measured directly by neutron or x-ray diffraction,[6] which can be constructed using the theory in this paper, which extends previous work[5] to further neighbors.

In Sec. II, we outline the theory for the generic random alloy, and present the results and discussion in Sec. III. The reader interested only in the results can proceed directly to Sec. III.

II. THEORETICAL FORMALISM

A. Lattice topology parameters

We assume that each kind of atomic species resides on a sublattice of an otherwise perfect zinc-blende structure. In the λ model,[7] the strain energy induced by the length-mismatch field $\{\mathbf{u}_l\}$ can be written as

$$V(\lambda)=\frac{1}{2}\alpha\sum_{\langle ll'\rangle}(L_e-L^0_{ll'}+\hat{\mathbf{r}}_{ll'}\cdot\mathbf{u}_{ll'})^2 + \frac{1}{8}\beta\sum_{\langle ll'l''\rangle}[\hat{\mathbf{r}}_{ll'}\cdot\mathbf{u}_{l''l'}+\hat{\mathbf{r}}_{l''l'}\cdot\mathbf{u}_{ll'} +\tfrac{1}{3}\lambda(\hat{\mathbf{r}}_{ll'}\cdot\mathbf{u}_{ll'}+\hat{\mathbf{r}}_{l''l'}\cdot\mathbf{u}_{l''l'})]^2 , \quad (1)$$

where we sum over all possible nearest-neighbor bonds and bond angles in the structure. When $\lambda=0$, we recover the Keating model;[8] and when $\lambda=1$, the Kirkwood model.[9]

For convenience, we introduce *two* sets of indicator functions[10] on each site of the two sublattices, such that if an atom at site i (on the A sublattice) is of the α type, f^i_α is 1, and 0 otherwise. Similarly g^j_β is defined on the B sublattice. Note that $\sum_\alpha f^i_\alpha=1$, and $\sum_\beta g^j_\beta=1$. In this language, if r^0_α and r^0_β are the natural (i.e., relaxed) radii of the α and β species, respectively, then the additivity of atomic radii means that the *natural* bond length L^0_{ij} can be written as

$$L^0_{ij}=\sum_{\alpha\beta}f^i_\alpha g^j_\beta L^0_{\alpha\beta} =\sum_{\alpha\beta}f^i_\alpha g^j_\beta(r^0_\alpha+r^0_\beta) =\sum_\alpha f^i_\alpha r^0_\alpha+\sum_\beta g^j_\beta r^0_\beta . \quad (2)$$

Therefore, in the linear approximation, two types of disorder-induced stress fields can be defined,

$$\phi_i=\alpha\sum_{j(i)}\hat{\mathbf{r}}_{ij}\sum_{\beta}g_{\beta}^{j}r_{\beta}^{0}\ , \tag{3a}$$

$$\phi_j=\alpha\sum_{i(j)}\hat{\mathbf{r}}_{ji}\sum_{\alpha}f_{\alpha}^{i}r_{\alpha}^{0}\ , \tag{3b}$$

where $\sum_{j(i)}$ denotes a sum over the four nearest neighbors of i, and so on. Notice that we have used the letter α both for the central nearest-neighbor force constant *and* as a subscript to indicate the chemical species on one sublattice. It is clear which is which by whether α is a subscript or not. Similar remarks apply to β.

In the Fourier space of the underlying fcc Bravais lattice, the dynamical matrix of the system can be block diagonalized (6×6). By minimizing the strain energy with respect to the internal displacement field, we obtain

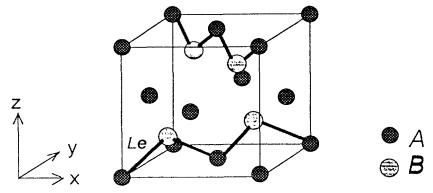

FIG. 1. Coordinate system as fixed by the underlying mean zinc-blende structure, where L_e is the nearest-neighbor bond length, and A an atom at the origin. The convention used in this paper is such that the nearest-neighbor B atoms are at $(1,1,1)L_e/\sqrt{3}$, $(-1,-1,1)L_e/\sqrt{3}$, $(-1,1,-1)L_e/\sqrt{3}$, and $(1,-1,-1)L_e/\sqrt{3}$.

$$\mathbf{D}_{\mathbf{k}}\begin{bmatrix}\mathbf{u}_{\mathbf{k}}^{(+)}\\ \mathbf{u}_{\mathbf{k}}^{(-)}\end{bmatrix}=\begin{bmatrix}\boldsymbol{\phi}_{\mathbf{k}}^{(+)}\\ \boldsymbol{\phi}_{\mathbf{k}}^{(-)}\end{bmatrix}\ , \tag{4a}$$

where

$$\begin{aligned}\mathbf{D}_{\mathbf{k}}=&\alpha\begin{bmatrix}\frac{4}{3}\mathbb{1} & -\tau_{-\mathbf{k}}\\ -\tau_{\mathbf{k}} & \frac{4}{3}\mathbb{1}\end{bmatrix}+\beta\begin{bmatrix}\frac{4}{3}\mathbb{1}+\frac{1}{4}\mathbf{v}_{\mathbf{k}}\mathbf{v}_{-\mathbf{k}} & \tau_{-\mathbf{k}}-\frac{2}{3}\gamma_{-\mathbf{k}}\mathbb{1}\\ \tau_{\mathbf{k}}-\frac{2}{3}\gamma_{\mathbf{k}}\mathbb{1} & \frac{4}{3}\mathbb{1}+\frac{1}{4}\mathbf{v}_{-\mathbf{k}}\mathbf{v}_{\mathbf{k}}\end{bmatrix}\\ &+\frac{1}{9}\beta\lambda\begin{bmatrix}\frac{4}{3}\mathbb{1}+\frac{1}{4}\mathbf{v}_{-\mathbf{k}}\mathbf{v}_{\mathbf{k}}+\frac{3}{4}\gamma_{\mathbf{k}}\tau_{-\mathbf{k}}+\frac{3}{4}\gamma_{-\mathbf{k}}\tau_{\mathbf{k}} & -\tau_{-\mathbf{k}}-2\gamma_{-\mathbf{k}}\mathbb{1}\\ -\tau_{\mathbf{k}}-2\gamma_{\mathbf{k}}\mathbb{1} & \frac{4}{3}\mathbb{1}+\frac{1}{4}\mathbf{v}_{\mathbf{k}}\mathbf{v}_{-\mathbf{k}}+\frac{3}{4}\gamma_{-\mathbf{k}}\tau_{\mathbf{k}}+12\gamma_{\mathbf{k}}\tau_{-\mathbf{k}}\end{bmatrix}\\ \equiv&\begin{bmatrix}\mathbf{D}_{\mathbf{k}}^{(++)} & \mathbf{D}_{\mathbf{k}}^{(+-)}\\ \mathbf{D}_{\mathbf{k}}^{(-+)} & \mathbf{D}_{\mathbf{k}}^{(--)}\end{bmatrix}\ ,\end{aligned} \tag{4b}$$

whose inverse defines the Green's function $\mathbf{G}_{\mathbf{k}}$ of the corresponding network. Note that both $\mathbf{D}_{\mathbf{k}}$ and $\mathbf{G}_{\mathbf{k}}$ are Hermitian, which is consistent with the strain energy being real. Here we use $+$ and $-$ to label the A and B sublattices, and for the coordinate system chosen (Fig. 1), we have

$$\gamma_{\mathbf{k}}\equiv\sum_{\delta}e^{-i\mathbf{k}\cdot\boldsymbol{\delta}}=4\left[\cos\left[\frac{k_xL_e}{\sqrt{3}}\right]\cos\left[\frac{k_yL_e}{\sqrt{3}}\right]\cos\left[\frac{k_zL_e}{\sqrt{3}}\right]+i\sin\left[\frac{k_xL_e}{\sqrt{3}}\right]\sin\left[\frac{k_yL_e}{\sqrt{3}}\right]\sin\left[\frac{k_zL_e}{\sqrt{3}}\right]\right]\ , \tag{5}$$

where L_e is the nearest-neighbor bond length. The vector $\mathbf{v}_{\mathbf{k}}$ and the tensor $\tau_{\mathbf{k}}$ are quantities derivable from $\gamma_{\mathbf{k}}$, that is, $\mathbf{v}_{\mathbf{k}}\equiv(i\nabla_{\mathbf{k}}/L_e)\gamma_{\mathbf{k}}$, $\tau_{\mathbf{k}}\equiv(i\nabla_{\mathbf{k}}/L_e)(i\nabla_{\mathbf{k}}L_e)\gamma_{\mathbf{k}}$, and $\mathbb{1}$ is used to denote the 3×3 unit matrix.

In this way, we may write, for example,

$$\begin{aligned}\mathbf{u}_i=&\sum_{\mathbf{k}}\mathbf{u}_{\mathbf{k}}^{(+)}e^{i\mathbf{k}\cdot\mathbf{i}}=\sum_{\mathbf{k}}(\mathbf{G}_{\mathbf{k}}^{(++)}\cdot\boldsymbol{\phi}_{\mathbf{k}}^{(+)}+\mathbf{G}_{\mathbf{k}}^{(+-)}\cdot\boldsymbol{\phi}_{\mathbf{k}}^{(-)})e^{i\mathbf{k}\cdot\mathbf{i}}\\ =&\alpha\sum_{\langle i'j''\rangle}\left[\frac{1}{N}\sum_{\mathbf{k}}\mathbf{G}_{\mathbf{k}}^{(++)}e^{i\mathbf{k}(\mathbf{i}-\mathbf{i}')}\right]\cdot\hat{\mathbf{r}}_{i'j''}\sum_{\beta}g_{\beta}^{j''}r_{\beta}^{0}+\alpha\sum_{\langle j'i''\rangle}\left[\frac{1}{N}\sum_{\mathbf{k}}\mathbf{G}_{\mathbf{k}}^{(+-)}e^{i\mathbf{k}\cdot(\mathbf{i}-\mathbf{j}')}\right]\cdot\hat{\mathbf{r}}_{j'i''}\sum_{\alpha}f_{\alpha}^{i''}r_{\alpha}^{0}\\ \equiv&\sum_{i'}\mathbf{G}_{ii'}\cdot\boldsymbol{\phi}_{i'}+\sum_{j'}\mathbf{G}_{ij'}\cdot\boldsymbol{\phi}_{j'}\ .\end{aligned} \tag{6}$$

This identifies the Green's function in real space: For any two points l,l' in the crystal, if $s_l,s_{l'}$ are their sublattice labels (where $s_l=\pm$, etc.), then

$$\mathbf{G}_{ll'}=\mathbf{G}_{l-l'}=\frac{1}{N}\sum_{\mathbf{k}}\mathbf{G}_{\mathbf{k}}^{(s_l,s_{l'})}e^{i\mathbf{k}\cdot(l-l')}\ . \tag{7}$$

Therefore, from Eqs. (6), (7), and (3), we can express the derivation of the bond length between *any* two sites, say i, and j, from its value L_{ij}^{e} in the underlying virtual crystal, in terms of the indicator functions. This will facilitate calculations of the bond-length distribution function and its various moments. Obviously, L_{ij}^{e} can be written in terms of L_e, the nearest-neighbor distance, times an appropriate geometric factor. For example, the next-nearest-neighbor distance $L_{nnn}=\sqrt{8/3}L_e$, where L_e is just the average bond length $\sum_{\alpha}x_{\alpha}r_{\alpha}^{0}+\sum_{\beta}y_{\beta}r_{\beta}^{0}$ [cf. Eq. (2)]. We have

$$L_{ij}-L^{e}_{ij}=\hat{\mathbf{r}}_{ij}\cdot\mathbf{u}_{ij}=\hat{\mathbf{r}}_{ij}\cdot(\mathbf{u}_i-\mathbf{u}_j)=\hat{\mathbf{r}}_{ij}\cdot\left[\sum_{i'}(\mathbf{G}_{i-i'}-\mathbf{G}_{j-i'})\cdot\boldsymbol{\phi}_{i'}+\sum_{j'}(\mathbf{G}_{i-j'}-\mathbf{G}_{j-j'})\cdot\boldsymbol{\phi}_{j'}\right]$$

$$=\sum_{i''}\left[\alpha\hat{\mathbf{r}}_{ij}\cdot\sum_{j'(i'')}(\mathbf{G}_{i-j'}-\mathbf{G}_{j-j'})\cdot\hat{\mathbf{r}}_{j'i''}\right]\sum_{\alpha}f^{i''}_{\alpha}r^{0}_{\alpha}+\sum_{j''}\left[\alpha\hat{\mathbf{r}}_{ij}\cdot\sum_{i'(j'')}(\mathbf{G}_{i-i'}-\mathbf{G}_{j-i'})\cdot\hat{\mathbf{r}}_{i'j''}\right]\sum_{\beta}g^{j''}_{\beta}r^{0}_{\beta}$$

$$\equiv\sum_{i''}a_{ij,i''}\sum_{\alpha}f^{i''}_{\alpha}r^{0}_{\alpha}+\sum_{j''}a_{ij,j''}\sum_{\beta}g^{j''}_{\beta}r^{0}_{\beta}\ . \tag{8}$$

This defines the three-point functions $a_{ij,i''}, a_{ij,j''}$, which depend only on the topology of the underlying virtual crystal lattice. Clearly, for any three lattice sites **l**, **m**, and **n**, $a_{mn,l}=a_{nm,l}$; and because of the zinc-blende symmetry, we also have $\sum_l a_{mn,l}=0$. Now, since a lattice site and its nearest neighbors always have the opposite sublattice labels, the three-point function can be further expressed in terms of a vector field, such that

$$a_{mn,l}=a_{m-l,n-l}=\hat{\mathbf{r}}_{mn}\cdot(\mathbf{V}_{m-l}-\mathbf{V}_{n-l})s_l\ , \tag{9a}$$

and

$$\mathbf{V}_{m-l}\equiv\frac{1}{N}\sum_{k}(\alpha\mathbf{G}_k^{(s_m,-s_l)}\cdot\mathbf{v}_{s_l k})e^{i\mathbf{k}\cdot(m-l)}\ . \tag{9b}$$

Physically, $\mathbf{V}_{m-l}$ represents the contribution to the displacement at site **m** from the nearest neighbors of site *l*, a quantity that depends only on the topology of the network. Obviously, $\mathbf{V}_0=\mathbf{0}$. However, it is important to note that, in general, $\mathbf{V}_{m-l}\neq\mathbf{V}_{l-m}$. This is because the local inversion symmetry is broken at the sites in the zinc-blende structure.

To be specific, let $\mathbf{V}_k^{(s_m,s_l)}$ be the Fourier component of the vector field; it then transforms exactly the same as **k** under the T_d operations. If z_k is the number of operations associated with **k**, then it can be shown that

$$\mathbf{V}_{m-l}=-\frac{1}{3N}\sum_{k}z_k\begin{bmatrix}\mathrm{Re}(V_k^{(s_m,s_l)})_x\cos\theta_x\sin\theta_y\sin\theta_z+\mathrm{Im}(V_k^{(s_m,s_l)})_x\sin\theta_x\cos\theta_y\cos\theta_z\\ \mathrm{Re}(V_k^{(s_m,s_l)})_y\sin\theta_x\cos\theta_y\sin\theta_z+\mathrm{Im}(V_k^{(s_m,s_l)})_y\cos\theta_x\sin\theta_y\cos\theta_z\\ \mathrm{Re}(V_k^{(s_m,s_l)})_z\sin\theta_x\sin\theta_y\cos\theta_z+\mathrm{Im}(V_k^{(s_m,s_l)})_z\cos\theta_x\cos\theta_y\sin\theta_z\end{bmatrix}\ , \tag{10}$$

where $\theta_x\equiv k_x(m_x-l_x)$, $\theta_y\equiv k_y(m_y-l_y)$, and $\theta_z\equiv(m_z-l_z)$. An inversion operation in **k** space will take $\mathbf{V}_k^{(s_m,s_l)}$ into its complex conjugate, which in turn is equivalent to exchanging the two sublattices: $\mathbf{V}_{-k}^{(s_m,s_l)}=(\mathbf{V}_k^{(s_m,s_l)})^*=\mathbf{V}_k^{(-s_m,-s_l)}$. It then follows that $\mathbf{V}_{j-i}=\mathbf{V}_{i-j}$, but $\mathbf{V}_{i'-i}\neq\mathbf{V}_{i-i'}$. Nonetheless, the effect may not be observable in either simulations or experiments, as we will be only concerned with the distance separating the two points of interest. For the zinc-blende structure, both $\mathbf{V}_{m-l}$ and $a_{m-l,n-l}$ can be readily calculated.

Equations (8) and (9) are the main results of this subsection. In the next subsection, we use these expressions to derive the bond-length distribution functions, and calculate the first two moments.

B. Bond-length distribution functions

The length distribution function for a chemically specific bond **ij** is defined as

$$P^{ij}_{\alpha\beta}(L)\equiv\langle f^{i}_{\alpha}g^{j}_{\beta}\delta(L-L_{ij})\rangle\ , \tag{11}$$

where $\langle\ \rangle$ denotes the statistical average over all possible configurations. Replacing the δ function by its integral form, we have

$$P^{ij}_{\alpha\beta}(L)=\frac{1}{2\pi}\int_{-\infty}^{\infty}dqF^{ij}_{\alpha\beta}(q)e^{iqL}\ , \tag{12a}$$

where

$$F^{ij}_{\alpha\beta}(q)\equiv\langle f^{i}_{\alpha}g^{j}_{\beta}e^{-iqL_{ij}}\rangle\ . \tag{12b}$$

Using Eq. (8) for L_{ij}, and noting that the occupancy statistics on the two sublattices are independent, we obtain a factorized form of the length-distribution function, each involving terms on a *single* sublattice

$$F^{ij}_{\alpha\beta}(q)=\left\langle f^{i}_{\alpha}g^{j}_{\beta}e^{-iq\left(L^{e}_{ij}+\sum_{i'}a_{ij,i'}\sum_{\alpha'}f^{i'}_{\alpha'}r^{0}_{\alpha'}+\sum_{j'}a_{ij,j'}\sum_{\beta'}g^{j'}_{\beta'}r^{0}_{\beta'}\right)}\right\rangle$$

$$=e^{-iqL^{e}_{ij}}\left\langle f^{i}_{\alpha}e^{-iq\sum_{i'}a_{ij,i'}\sum_{\alpha'}f^{i'}_{\alpha'}r^{0}_{\alpha'}}\right\rangle\left\langle g^{j}_{\beta}e^{-iq\sum_{j'}a_{ij,j'}\sum_{\beta'}g^{j'}_{\beta'}r^{0}_{\beta'}}\right\rangle\ . \tag{13}$$

It is straightforward to see that, at any site **i**, $f^{i}_{\alpha}f^{i}_{\alpha'}=\delta_{\alpha\alpha'}f^{i}_{\alpha}$, while at any two different sites **i** and **i'**, f^{i}_{α} and $f^{i'}_{\alpha'}$ are sta-

tistically independent. This means that the ensemble averages in the above equation can be explicitly calculated. We have

$$\left\langle f_\alpha^{\mathbf{i}} e^{-iq\sum_{\mathbf{i}'} a_{\mathbf{ij},\mathbf{i}'} \sum_{\alpha'} f_{\alpha'}^{\mathbf{i}'} r_{\alpha'}^0} \right\rangle = \left\langle f_\alpha^{\mathbf{i}} \prod_{\mathbf{i}',\alpha'} [1+f_{\alpha'}^{\mathbf{i}'}(e^{-iqa_{\mathbf{ij},\mathbf{i}'} r_{\alpha'}^0}-1)] \right\rangle$$

$$= \left\langle f_{\alpha'}^{\mathbf{i}} \prod_{\alpha'} [1+f_\alpha^{\mathbf{i}}(e^{-iqa_{\mathbf{ij},\mathbf{i}'} r_{\alpha'}^0}-1)] \prod_{\mathbf{i}'(\neq\mathbf{i}),\alpha'} [1+f_{\alpha'}^{\mathbf{i}'}(e^{-iqa_{\mathbf{ij},\mathbf{i}'} r_{\alpha'}^0}-1)] \right\rangle$$

$$= x_\alpha e^{-iqa_{\mathbf{ij},\mathbf{i}} r_\alpha^0} \prod_{\mathbf{i}'(\neq\mathbf{i})} \left[1+\sum_{\alpha'} x_{\alpha'}(e^{-iqa_{\mathbf{ij}\cdot\mathbf{j}'} r_{\alpha'}^0}-1) \right] ; \tag{14a}$$

similarly,

$$\left\langle g_\beta^{\mathbf{j}} e^{-iq\sum_{\mathbf{j}'} a_{\mathbf{ij},\mathbf{j}'} \sum_{\beta'} g_{\beta'}^{\mathbf{j}'} r_{\beta'}^0} \right\rangle = y_\beta e^{-iqa_{\mathbf{ij},\mathbf{j}} r_\beta^0} \prod_{\mathbf{j}'(\neq\mathbf{j})} \left[1+\sum_{\beta'} y_{\beta'}(e^{-iqa_{\mathbf{ij},\mathbf{j}'} r_{\beta'}^0}-1) \right] . \tag{14b}$$

Therefore

$$F_{\alpha\beta}^{\mathbf{ij}}(q) = x_\alpha y_\beta e^{-iq(L_{\mathbf{ij}}^e + a_{\mathbf{ij},\mathbf{i}} r_\alpha^0 + a_{\mathbf{ij},\mathbf{j}} r_\beta^0)} f_{\mathbf{ij}}(q) , \tag{15a}$$

and $f_{\mathbf{ij}}(q)$ is a universal function independent of the particular type of atoms at sites $\mathbf{i},\mathbf{j}$ in question, as it does not to involve α or β, and has the form

$$f_{\mathbf{ij}}(q) \equiv \prod_{\mathbf{i}'(\neq\mathbf{i})} \left[1+\sum_{\alpha'} x_{\alpha'}(e^{-iqa_{\mathbf{ij},\mathbf{i}'} r_{\alpha'}^0}-1) \right] \prod_{\mathbf{j}'(\neq\mathbf{j})} \left[1+\sum_{\beta'} y_{\beta'}(e^{-iqa_{\mathbf{ij},\mathbf{j}'} r_{\beta'}^0}-1) \right] . \tag{15b}$$

From the distribution function Eqs. (15), we can derive the average length between *any* two sites, say $\mathbf{i}$ and $\mathbf{j}$. It is not hard to see that $P_{\alpha\beta}^{\mathbf{ij}}(L)$ is normalized to $x_\alpha y_\beta$, and its first moment gives the averaged bond length between two chemically specific sites (i.e., keeping the concentration of the α species fixed at site $\mathbf{i}$, and that of the β species fixed at site $\mathbf{j}$, while allowing the rest of the system to go over all its possible configurations), we have

$$\langle L_{\mathbf{ij}}^{\alpha\beta} \rangle = i\frac{\partial}{\partial q} \left[\frac{F_{\alpha\beta}^{\mathbf{ij}}(q)}{x_\alpha y_\beta} \right] \Bigg|_{q=0} = L_{\mathbf{ij}}^e + a_{\mathbf{ij},\mathbf{i}} \left[r_\alpha^0 - \sum_{\alpha'} x_{\alpha'} r_{\alpha'}^0 \right] + a_{\mathbf{ij},\mathbf{j}} \left[r_\beta^0 - \sum_{\beta'} y_{\beta'} r_{\beta'}^0 \right] , \tag{16}$$

where we have used the summation rule $\sum_{\mathbf{i}'} a_{\mathbf{ij},\mathbf{i}'} = 0$, and so on.

Similarly, the fluctuation of the bond length from its mean value (due to randomness) is given by the second moment of $P_{\alpha\beta}^{\mathbf{ij}}(L)$. We obtain

$$\langle (L_{\mathbf{ij}}^{\alpha\beta} - \langle L_{\mathbf{ij}}^{\alpha\beta} \rangle)^2 \rangle = -\frac{\partial^2}{\partial q^2} \left[\frac{F_{\alpha\beta}^{\mathbf{ij}}(q)}{x_\alpha y_\beta e^{-iq\langle L_{\mathbf{ij}}^{\alpha\beta} \rangle}} \right] \Bigg|_{q=0}$$

$$= \sum_{\mathbf{i}'(\neq\mathbf{i})} a_{\mathbf{ij},\mathbf{i}'}^2 \left[\sum_{\alpha'} x_{\alpha'}(r_{\alpha'}^0)^2 - \left[\sum_{\alpha'} x_{\alpha'} r_{\alpha'}^0 \right]^2 \right] + \sum_{\mathbf{j}'(\neq\mathbf{j})} a_{\mathbf{ij},\mathbf{j}'}^2 \left[\sum_{\beta'} y_{\beta'}(r_{\beta'}^0)^2 - \left[\sum_{\beta'} y_{\beta'} r_{\beta'}^0 \right]^2 \right] . \tag{17}$$

Thus, the second moment is independent of the atomic species α and β, which is also true of all higher order of moments. Therefore, the shape of the length-distribution function, when properly weighted and shifted, is independent of the atomic species at the two sites, as mentioned previously.

For completeness, we record below the expressions for the case where the two sites are of the same (A) type. We have

$$\langle L_{\mathbf{ii}'}^{\alpha\alpha'} \rangle = L_{\mathbf{ii}'}^e + a_{\mathbf{ii}',\mathbf{i}} \left[r_\alpha^0 - \sum_{\alpha''} x_{\alpha''} r_{\alpha''}^0 \right] + a_{\mathbf{ii}',\mathbf{i}'} \left[r_{\alpha'}^0 - \sum_{\alpha''} x_{\alpha''} r_{\alpha''}^0 \right] , \tag{18}$$

and

$$\langle (L_{\mathbf{ii}'}^{\alpha\alpha'} - \langle L_{\mathbf{ii}'}^{\alpha\alpha'} \rangle)^2 \rangle = \sum_{\mathbf{i}''(\neq\mathbf{i},\mathbf{i}')} a_{\mathbf{ii}',\mathbf{i}''}^2 \left[\sum_{\alpha''} x_{\alpha''}(r_{\alpha''}^0)^2 - \left[\sum_{\alpha''} x_{\alpha''} r_{\alpha''}^0 \right]^2 \right] + \sum_{\mathbf{j}} a_{\mathbf{ii}',\mathbf{j}}^2 \left[\sum_{\beta} y_\beta (r_\beta^0)^2 - \left[\sum_{\beta} y_\beta r_\beta^0 \right]^2 \right] . \tag{19}$$

Equations (16)–(19) are the central results of this paper. For values of β/α and λ [see Eq. (1)] the coefficients in (16)–(19) can be readily computed using the Monte Carlo integration method in Fourier space. The expressions can be further simplified by using Eqs. (9) and (10). Note that in both simulations and PDF experiments, we are only concerned with the relative distance (scalar) between any two sites, not their relative orientation (vector). Thus, in addition to the statistical averages taken so far, we may also average over bond orientations. The results are presented in Sec. III.

III. RESULTS AND DISCUSSION

We summarize below the main results of this paper. Let i,i′ be any two points on the A sublattice, and j be a point on the B sublattice, then the *statistically* averaged bond-length deviations and fluctuations are

$$\langle L_{\mathbf{ij}}^{\alpha\beta}\rangle - L_{\mathbf{ij}}^{e} = a_{AB}^{**}(\mathbf{ij})(\Delta_\alpha+\Delta_\beta)\ , \tag{20a}$$

$$\langle (L_{\mathbf{ij}}^{\alpha\beta}-\langle L_{\mathbf{ij}}^{\alpha\beta}\rangle)^2\rangle = b_{AB}^{**}(\mathbf{ij})(\sigma_A^2+\sigma_B^2)\ , \tag{20b}$$

$$\langle L_{\mathbf{ii'}}^{\alpha\alpha'}\rangle - L_{\mathbf{ii'}}^{e} = a_{AA}^{**}(\mathbf{ii'})(\Delta_\alpha+\Delta_{\alpha'})\ , \tag{20c}$$

$$\langle (L_{\mathbf{ii'}}^{\alpha\alpha'}-\langle L_{\mathbf{ii'}}^{\alpha\alpha'}\rangle)^2\rangle = b_{AA,A}^{**}(\mathbf{ii'})\sigma_A^2 + b_{AA,B}^{**}(\mathbf{ii'})\sigma_B^2\ , \tag{20d}$$

where $\Delta_\alpha \equiv r_\alpha^0 - \sum_{\alpha''} x_{\alpha''} r_{\alpha''}^0$, $\sigma_A^2 \equiv \sum_{\alpha''} x_{\alpha''} (r_{\alpha''}^0)^2 - (\sum_{\alpha''} x_{\alpha''} r_{\alpha''}^0)^2$, and so on. Here, $L_{\mathbf{ij}}^{e}$ is the virtual lattice distance between sites i and j on *different* sublattices, and $L_{\mathbf{ii'}}^{e}$ that between i and i′ on the *same* sublattice. Explicitly, we have for the topological rigidity parameters

$$a_{AB}^{**}(\mathbf{ij}) = \hat{\mathbf{r}}_{\mathbf{ji}}\cdot\mathbf{V}_{\mathbf{ji}}\ , \tag{21a}$$

$$b_{AB}^{**}(\mathbf{ij}) = \sum_{\mathbf{i'}(\neq\mathbf{i})} [\hat{\mathbf{r}}_{\mathbf{ji}}\cdot(\mathbf{V}_{\mathbf{ji'}}-\mathbf{V}_{\mathbf{ii'}})]^2\ , \tag{21b}$$

$$a_{AA}^{**}(\mathbf{ii'}) = \tfrac{1}{2}\hat{\mathbf{r}}_{\mathbf{i'i}}\cdot(\mathbf{V}_{\mathbf{i'i}}-\mathbf{V}_{\mathbf{ii'}})\ , \tag{21c}$$

$$b_{AA,A}^{**}(\mathbf{ii'}) = \sum_{\mathbf{i''}(\neq\mathbf{i},\mathbf{i'})} [\hat{\mathbf{r}}_{\mathbf{i'i}}\cdot(\mathbf{V}_{\mathbf{i'i''}}-\mathbf{V}_{\mathbf{ii''}})]^2\ , \tag{21d}$$

$$b_{AA,B}^{**}(\mathbf{ii'}) = \sum_{j} [\hat{\mathbf{r}}_{\mathbf{i'i}}\cdot(\mathbf{V}_{\mathbf{i'j}}-\mathbf{V}_{\mathbf{ij}})]^2\ , \tag{21e}$$

where the **V**'s are defined through Eqs. (9b) and (7). For a given separation R, these topological rigidity parameters can be easily calculated by the Monte Carlo integration method, i.e., sampling the **k** space with large numbers of points. It should be clear that the model parameters α and β in Eq. (1) enter these expressions only through the combination β/α.

We show in Fig. 2 the values of a_{AB}^{**} (open circles) and a_{AA}^{**} (solid circles) out to the tenth neighbor, for $\beta/\alpha=0.2$, as calculated in the Kirkwood model. The crosses in Fig. 2 indicate the data points extracted from simulations on Si_xGe_{1-x}, with $x=0.3$. These simulation results were obtained by relaxing statically, using the Kirkwood potential given in Eq. (1), a supercell containing 110 592 atoms with Si and Ge distributed randomly. The topological rigidity parameters were extracted using

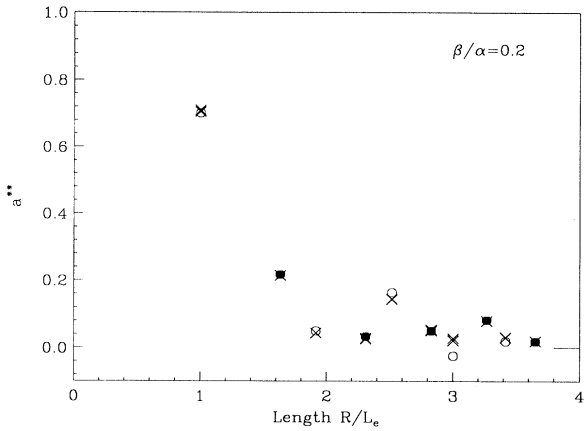

FIG. 2. Topological rigidity parameters a_{AB}^{**} and a_{AA}^{**} as functions of separation R, calculated for $\beta/\alpha=0.2$ in the Kirkwood model. The open circles are the a_{AB}^{**}'s, where the end points are on different sublattices, while the solid circles are the a_{AA}^{**}'s, in which both end points are on the same sublattice. Crosses are the data points extracted from simulations on $Si_{0.3}Ge_{0.7}$. At large R, both a_{AB}^{**} and a_{AA}^{**} approach zero, as indicated by the horizontal bar on the panel.

Eqs. (20). The agreement shown in Fig. 2 is excellent within some numerical fluctuations. Note that all the topological rigidity parameters in Eqs. (21) are independent of any particular compound or composition and in this sense are universal. In Fig. 3, we show the plot for b_{AB}^{**} (open circles), $b_{AA,A}^{**}$ (solid squares), and $b_{AA,B}^{**}$ (solid diamonds) as calculated in the general case, whereas for the

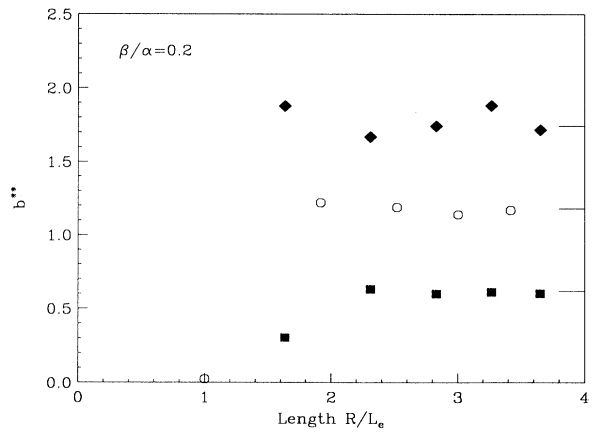

FIG. 3. Topological rigidity parameters b_{AB}^{**}, $b_{AA,A}^{**}$, and $b_{AA,B}^{**}$ as function of separation R, calculated for $\beta/\alpha=0.2$ in the Kirkwood model. The open circles are the b_{AB}^{**}'s, where the end points are on different sublattices. The solid squares are the $b_{AA,A}^{**}$'s, and the solid diamonds are the $b_{AA,B}^{**}$'s. These are quantities associated with the case in which the two end points are on the same sublattice. The limiting values of these parameters at large R are shown as horizontal bars.

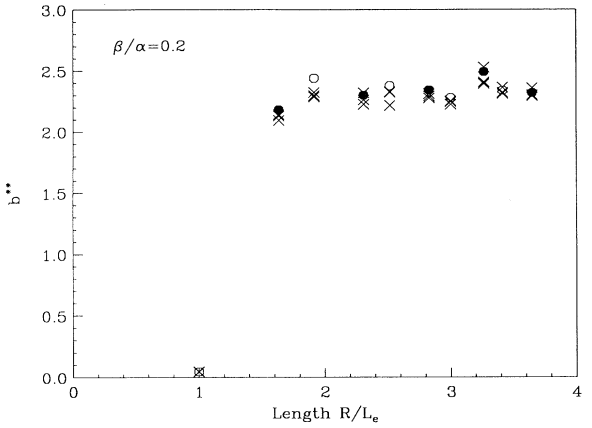

FIG. 4. Comparison of results from simulations on $Si_{0.3}Ge_{0.7}$ with theory for the topological rigidity parameter b^{**}'s obtained from the *widths* of the length-distribution functions, calculated for $\beta/\alpha=0.2$ in the Kirkwood model. Crosses are for Si-Si, Si-Ge, Ge-Ge pairs from simulations, and the circles are from theory.

Si_xGe_{1-x} alloy used in simulations, the latter two combine [cf. Eq. 20(d)]. A similar comparison is then given in Fig. 4, where the agreement is again excellent. In this figure, each theoretical point corresponds to three simulation points, drawn from Si-Si, Si-Ge, and Ge-Ge pairs. The fact that they overlap more or less on top of each other is a direct verification of the theory.

We observe that at a few neighbors away, both a^{**}_{AB} and a^{**}_{AA} decay rapidly to zero; while b^{**}_{AB}, $b^{**}_{AA,A}$, and $b^{**}_{AA,B}$ all approach the same asymptotic value, the mean-square strain-induced $\langle u^2 \rangle$, a quantity related to the disordered-induced Debye-Waller factor.[11] These

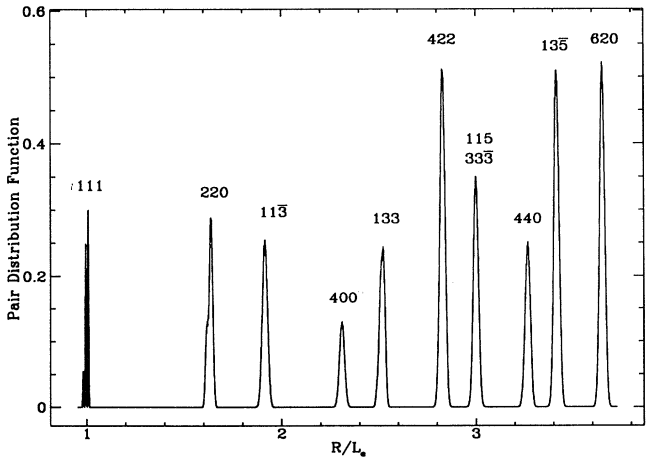

FIG. 5. Pair distribution function from simulations on $Si_{0.3}Ge_{0.7}$ vs distance R, calculated for $\beta/\alpha=0.2$ in the Kirkwood model. The subpeaks can be seen for the first two peaks, but not for more distant neighbors.

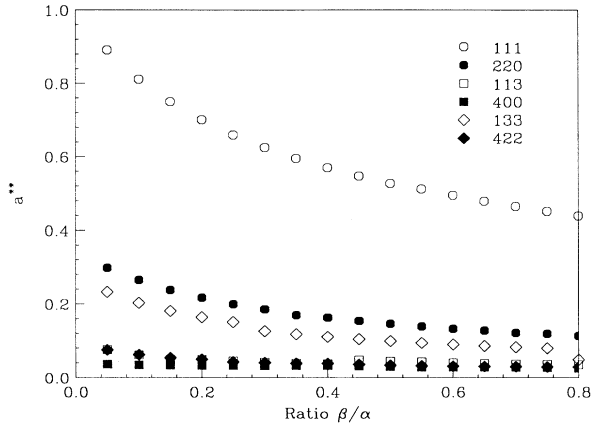

FIG. 6. Variations of a^{**}_{AB} and a^{**}_{AA} as functions of ratio β/α in the Kirkwood model.

limiting values are indicated as horizontal bars in Figs. 2 and 3. Thus, for a few neighbors away from a reference point in the alloy, the PDF as calculated in simulations, will have their peaks centered around the virtual lattice points, and their shapes approach a Gaussian with the same width (Fig. 5).

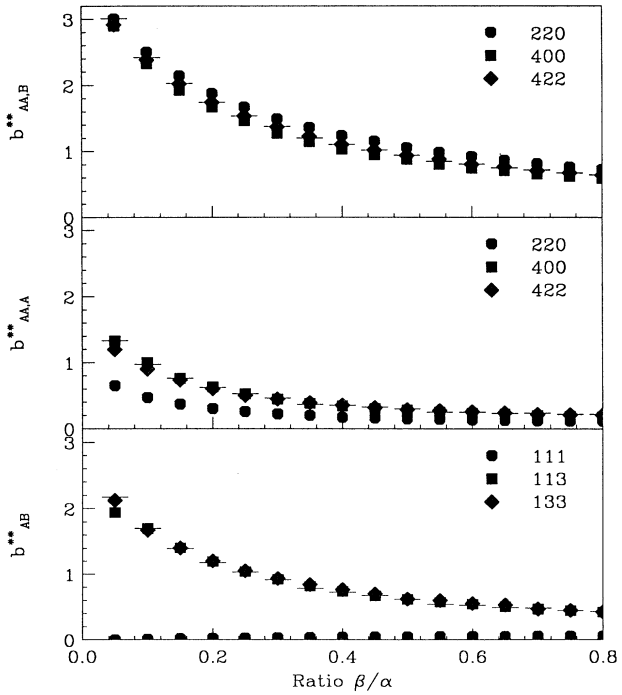

FIG. 7. Variations of b^{**}_{AB} (bottom panel), $b^{**}_{AA,A}$ (middle panel), and $b^{**}_{AA,B}$ (top panel) as functions of the ratio β/α in the Kirkwood model. The horizontal bars show the limiting values at large separations for fixed values at large separations for fixed values of β/α.

Variations of the topological rigidity parameters with the ratio β/α are shown in Figs. 6 and 7. For semiconductor alloys, $\beta/\alpha \approx 0.1-0.2$, and we list below (Table I) values of these parameters as functions of β/α, which will be of interest for particular alloys.

The topological rigidity parameters defined in previous work[5] are related to our present notation in the following manner:

$$a^{**}=a_{AB}^{**}(111)\ , \tag{22a}$$

$$b^{**}=\sqrt{\tfrac{8}{3}}a_{AA}^{**}(220)\ , \tag{22b}$$

$$a_1^{**}-a^{**2}=b_{AB}^{**}(111)\ , \tag{22c}$$

where we use the indices 111 and 220 to denote the nearest- and the next-nearest-neighbor shells in real-space (Fig. 1).

An example of a direct application of the current theory would be to consider the semimagnetic semiconducting alloy $Cd_{1-x-y}Mn_xZn_yTe$,[4,12] where the mean nearest-neighbor distance is given by $L_e=(1-x-y)L_{CdTe}^0+xL_{MnTe}^0+yL_{ZnTe}^0$, and the next-nearest-neighbor distance $L_{nnn}=\sqrt{\frac{8}{3}}L_e$. Here $L_{CdTe}^0=2.805$ Å, $L_{MnTe}^0=2.911$ Å, and $L_{ZnTe}^0=2.642$ Å. For magnetic properties, an important length is the mean spacing between the Mn pairs that are next nearest neighbors on the zinc-blende lattice. From Eqs. (20c) and (22b), this distance is given by

$$\begin{aligned} d(x,y)&\equiv L_{nnn}^{MnMn}\\ &=L_{nnn}+2a_{AA}^{**}(L_{nnn})(L_{MnTe}^0-L_e)\\ &=L_{nnn}+\sqrt{\tfrac{3}{2}}b^{**}(L_{MnTe}^0-L_e)\ , \end{aligned} \tag{23a}$$

or more explicitly

$$\begin{aligned} d(x,y)&=\sqrt{\tfrac{8}{3}}[(1-\tfrac{3}{4}b^{**})L_e+\tfrac{3}{4}b^{**}L_{MnTe}^0]\\ &=\sqrt{\tfrac{8}{3}}\{(1-\tfrac{3}{4}b^{**})[(1-x-y)L_{CdTe}^0+xL_{MnTe}^0+yL_{ZnTe}^0]+\tfrac{3}{4}b^{**}L_{MnTe}^0\}\\ &\equiv a+bx+cy\ . \end{aligned} \tag{23b}$$

The topological rigidity constant b^{**} has been found to be very close to (and not rigorously equal to) $a^{**}/2$ for all relevant values of β/α, and varies a little depending on the semiconductor, but is always about 0.4 in the Kirkwood model.[5] This gives $a=46324$ Å, $b=0.1210$ Å, and $c=-1.1863$ Å. Note that the linear combination of x and y that appears in $d(x,y)$ is independent of the precise value of b^{**}, as both have the same prefactor.

TABLE I. Topological rigidity parameters (labeled by the appropriate real-space indices) as functions of β/α in the range of practical interest (Kirkwood model).

β/α	0.05	0.10	0.15	0.20	0.25
$a_{AB}^{**}(111)$	0.891	0.811	0.750	0.700	0.659
$b_{AB}^{**}(111)$	0.00384	0.0103	0.0178	0.0240	0.0294
$a_{AA}^{**}(220)$	0.298	0.265	0.237	0.217	0.199
$b_{AA},A^{**}(220)$	0.649	0.467	0.368	0.303	0.258
$b_{AA},B^{**}(220)$	3.01	2.50	2.14	1.88	1.67
$a_{AB}^{**}(11\bar{3})$	0.0757	0.0616	0.0494	0.0495	0.0451
$b_{AB}^{**}(11\bar{3})$	1.94	1.69	1.40	1.20	1.04
$a_{AA}^{**}(400)$	0.0360	0.0341	0.0334	0.0331	0.0327
$b_{AA,A}^{**}(400)$	1.32	0.998	0.759	0.631	0.521
$b_{AA,B}^{**}(400)$	2.90	2.33	1.93	1.67	1.47
$a_{AB}^{**}(133)$	0.232	0.202	0.180	0.164	0.150
$b_{AB}^{**}(133)$	2.12	1.68	1.40	1.21	1.05
$a_{AA}^{**}(42\bar{2})$	0.0752	0.0624	0.0537	0.0497	0.0428
$b_{AA},A^{**}(42\bar{2})$	1.20	0.901	0.734	0.600	0.508
$b_{AA},B^{**}(42\bar{2})$	2.92	2.38	2.02	1.74	1.53

IV. SUMMARY

We have generalized previous results for binary and pseudobinary alloys to general semiconductor alloys with the zinc-blende structure. These alloys contain an arbitrary number of chemical species on each sublattice that form a random solid solution. We have not considered clustering.

We have shown that the length probability distribution for a particular pair of sites is independent of the chemical species, apart from the weight and centroid position. We have given general expressions for the mean length and width of the probability distribution for particular chemical pairs, an arbitrary distance apart. All the results are expressed in terms of a few topological rigidity parameters which are given numerically for the Kirkwood model.

Some structural information in semiconductor alloys can be obtained by x-ray absorption fine structure, but this is restricted to next-nearest-neighbor and occasionally second-nearest-neighbor distances.[2] Widths and further neighbor information will have to await very careful pair distribution function diffraction experiments with x rays or neutrons on powdered samples.[13]

ACKNOWLEDGMENTS

We thank F. Jacobs for useful discussions on $Cd_{1-x-y}Mn_xZn_yTe$, and the NSF for partial support under Grant No. CHE-92-24102.

[1]L. Végard, Z. Phys. **5**, 17 (1921).
[2]J. C. Mikkelsen, Jr. and J. B. Boyce, Phys. Rev. B **28**, 7130 (1983); Phys. Rev. Lett. **49**, 1412 (1982); J. B. Boyce and J. C. Mikkelsen, Jr., Phys. Rev. B **31**, 6903 (1985).
[3]A. Balzarotti, in *Theory and Multinary Compounds,* edited by S. K. Deb and A. Zunger (Materials Research Society, Pittsburgh, 1987), p. 333.
[4]F. Jacobs, Ph.D. thesis, Purdue University, 1995.
[5]Y. Cai and M. F. Thorpe, Phys. Rev. B **46**, 15 872 (1992); **46**, 15 879 (1992); N. Mousseau and M. F. Thorpe, *ibid.* **46**, 15 887 (1992).
[6]B. E. Warren, *X-ray Diffraction* (Addison-Wesley, Reading, 1969); H. P. Klug and L. E. Alexander, *X-ray Diffraction Procedures for Polycrystalline and Amorphous Materials* (Wiley, New York, 1968); T. Egami, Mater. Trans. **31**, 163 (1990).
[7]Y. Cai, Ph.D. thesis, Michigan State University, 1991.
[8]P. N. Keating, Phys. Rev. **145**, 637 (1966).
[9]J. G. Kirkwood, J. Chem. Phys. **7**, 506 (1939).
[10]P. A. P. Moran, *An Introduction to Probability Theory* (Oxford University Press, Oxford, 1968).
[11]M. F. Thorpe, J. S. Chung, and Y. Cai, Phys. Rev. B **43**, 8282 (1991).
[12]Structural and electornic properties of the pseudoternary alloy $Cd_{1-x-y}Mn_xZn_yTe$ are measured and discussed by R. Brun Del Re, T. Donofrio, J. Avon, J. Majid, and J. C. Woolley, Nuovo Cimento **2D**, 1911 (1982).
[13]S. Billinge (private communication).